

**(E,E'N) AND (E,E'NN) EXPERIMENTS AT NIKHEF, MAINZ
AND JLAB AND OPEN PROBLEMS IN ONE- AND
TWO-NUCLEON EMISSIONS**

S. BOFFI

*Dipartimento di Fisica Nucleare e Teorica, Università degli Studi di Pavia, and
Istituto Nazionale di Fisica Nucleare, Sezione di Pavia, I-27100 Pavia, Italy*

A critical review is presented of recent data on direct one- and two-nucleon emission obtained in electron scattering at NIKHEF, Mainz and JLab. In the case of $(e,e'p)$ reactions attention is focussed on extracting spectroscopic factors, looking at medium effects on the bound nucleon form factors, and investigating nuclear transparency. The possibility of obtaining information on nucleon-nucleon correlations in $(e,e'pp)$ and $(e,e'pn)$ reactions is also discussed.

1 Introduction

Electron scattering has been used for many years as a clean tool to explore nuclear structure. In the one-photon-exchange approximation, where the incident electron exchanges a photon of momentum \vec{q} and energy ω with the target, the response of atomic nuclei as a function of $Q^2 = |\vec{q}|^2 - \omega^2$ and ω can nicely be separated because the electromagnetic probe and its interaction are well under control. In addition, in direct one- and two-nucleon emission one may access to the single-particle properties of nuclei and nucleon-nucleon correlations, respectively (see, e.g., Ref. ¹).

In recent years, a great amount of data have been collected in laboratories in Europe and the USA.

The Amsterdam Pulse Stretcher and Storage-ring facility (AmPS) at the Dutch National Institute for Nuclear Physics and High-Energy Physics (NIKHEF) entered the phase of regular operations in 1993 providing beams of longitudinally polarized electrons of 900 MeV with stored currents of 150 mA and a state-of-the-art experimental facility with high-density, polarized internal targets. After a short period of intense and qualified work the AmPS facility has been decommissioned in January 1999 due to budgetary constraints and following the decision of the Dutch Research Council. Some part of the physics programme, such as the two-nucleon emission programme, together with some parts of the detectors, such as the Hadron3 detector originally designed to study reactions with a small cross section, has been transferred to Mainz.

In Mainz electron scattering experiments are performed by the A1 col-

laboration using a three-spectrometer setup to detect one or two charged particles in coincidence with the scattered electron coming from the 855 MeV (polarized) beam of the MAMI racetrack microtron. An upgrade to 1.6 GeV (MAMI-C) is under development and the new complex is planned to run in Spring 2004. ^a For the present purposes the experiments on (e,e'pp) and (e,e'pn) proposed under Refs. ^{2,3}, respectively, as well as the completed experiment (e,e'p) under Ref. ⁴ will be considered.

In the USA, besides the MIT-Bates laboratory operating with its 1 GeV electron beam, the Jefferson Laboratory (JLab) in Newport News, Virginia, began conducting experiments in November 1995 with its high-energy beams (up to 6 GeV at present, with possible upgrade to 12 GeV) of the Continuous Electron Beam Accelerator Facility (CEBAF). One-proton emission in electron scattering off a complex nucleus is studied in Halls A and C. In Hall A cross sections of charged particles detected in coincidence with the scattered electron can be measured with high precision with the available two identical High-Resolution Spectrometers. In Hall C a variety of experiments requiring high luminosity, but moderate resolution, is possible with the High-Momentum Spectrometer and the Short-Orbit Spectrometer. ^b Among others, of relevance here are the (e,e'p) experiments ^{5,6,7,8} in Hall A, as well as the proposal under Ref. ⁹ in Hall C and some corresponding results ^{10,11}. The proposal by van den Brand *et al.*¹² in Hall A will extend the Mainz data of Ref. ⁴ from $Q^2 = 0.8$ to 4.0 GeV².

In this review attention will be drawn to open problems more than to a successful interpretation of data.

2 (e,e'N)

In plane-wave impulse approximation (PWIA), i.e. neglecting final-state interactions (FSI) of the ejected particle, the coincidence (e,e'p) cross section in the one-photon exchange approximation is factorized ^{1,13} as a product of the (off-shell) electron-nucleon cross section σ_{eN} and the nuclear spectral density,

$$S(\vec{p}, E) = \sum_{\alpha} S_{\alpha}(E) |\phi_{\alpha}(\vec{p})|^2. \quad (1)$$

^aAn overview of approved experiments and accepted proposals can be obtained at the following web site: <http://www.a1.kph.uni-mainz.de/A1/proposals.html>.

^bA full list of approved experiments can be found at the following web sites for Hall A and Hall C, respectively: <http://www.jlab.org/exp-prog/generated/apphalla.html>, <http://www.jlab.org/exp-prog/generated/apphalc.html>.

At each removal energy E the \vec{p} dependence of $S(\vec{p}, E)$ is given by the momentum distribution of the quasi-hole states α produced in the target nucleus at that energy and described by the (normalized) overlap functions ϕ_α between the target (A -particle) nucleus ground state and the $(A - 1)$ -particle states of the residual nucleus. The spectroscopic factor S_α gives the probability that the such a quasi-hole state α be a pure hole state in the target nucleus. In an independent-particle shell model (IPSM) ϕ_α are just the single-particle states of the model, and $S_\alpha = 1(0)$ for occupied (empty) states. In reality, the strength of a quasi-hole state is fragmented over a set of single-particle states due to correlations, and $0 \leq S_\alpha < 1$.

With FSI such a factorization in the cross section is no longer possible, but in the past data were always organized in bins characterized by $|\vec{p}|$ and E by on-line dividing the counting rates by (a model dependent) σ_{eN} . Thus a five-fold cross section was converted into a two-fold reduced cross section and compared with a (distorted) spectral density $S^D(|\vec{p}|, E)$ including FSI described by an optical model potential. In the discrete spectrum of the residual nucleus at each excitation energy the $|\vec{p}|$ dependence of the reduced cross section is given by the corresponding model quasi-hole state and the normalization factor necessary to adjust $S^D(|\vec{p}|, E)$ to data is interpreted as the value of the spectroscopic factor extracted from experiment.

2.1 Spectroscopic factors and relativistic effects

Two major findings came out of these studies. First, the valence quasi-hole states ϕ_α almost overlap the IPSM functions with only a slight ($\sim 10\%$) enlargement of their rms radius. Second, a systematic suppression of the single-particle strength of valence states as compared to IPSM has been observed all over the periodic table. A quenching of spectroscopic factors is naturally conceived in nuclear many-body theory in terms of nucleon-nucleon correlations. However, model calculations produce spectroscopic factors S_α much larger than those extracted in low-energy ($e, e' p$) data. As an example, for the p-shell holes in ^{16}O a Green function approach to the spectral density ¹⁴ gives $S_{p_{1/2}} = 0.890$ and $S_{p_{3/2}} = 0.914$, while from experiment one has $S_{p_{1/2}} = 0.644$ and $S_{p_{3/2}} = 0.537$. A recent reanalysis ¹⁵ of the $^{12}\text{C}(e, e' p)$ data at $Q^2 \leq 0.3$ GeV² has found a very substantial reduction of the s- and p-shell strength by the factor 0.57 ± 0.02 .

In fact, the most general form of the coincidence cross section in the one-photon-exchange approximation is the contraction of a lepton tensor $L_{\mu\nu}$ with a hadron tensor $W^{\mu\nu}$ and involves nine structure functions ^{1,13}, that describe the response of the target system to the absorption of a longitudinal (L) or

transverse (T) photon. Each individual structure function is a bilinear form of the hadron current J^μ , i.e.

$$J^\mu = \int d\vec{r} \overline{\Psi}_f(\vec{r}) j^\mu(\vec{r}) e^{i\vec{q}\cdot\vec{r}} \Psi_i(\vec{r}), \quad (2)$$

where the charge-current operator $j^\mu(\vec{r})$ is responsible for the transition from an initial state $\Psi_i(\vec{r})$ (describing the motion of the ejected nucleon in its initial bound state) to a final state Ψ_f with the ejectile undergoing FSI with the residual nucleus. A complete separation of the various structure functions with appropriate (out-of-plane) kinematics would provide useful constraints when modelling the hadron current.

In the nonrelativistic PWIA approach, $\Psi_i(\vec{r})$ is identified with $[S_\alpha]^{1/2} \phi_\alpha(\vec{r})$ and Ψ_f becomes a plane wave. When including FSI according to an approach based on the distorted-wave impulse approximation (DWIA) and followed in the past in connection with low- Q^2 data, Ψ_f is taken as a solution to a Schrödinger equation for the ejectile in the field of the optical model potential produced by the residual nucleus. Uncertainties arise because phase-shift equivalent potentials for elastic proton-nucleus scattering do not in general give the same result for Ψ_f in the nucleus interior.

Ambiguities also arise in the definition of $j^\mu(\vec{r})$ that are related to current conservation and off-shell behaviour^{16,17}. Under quasi-free conditions the Coulomb gauge, where $J^3 = (\omega/|\vec{q}|) J^0$, and the Weyl gauge, where $J^0 = (|\vec{q}|/\omega) J^3$, give almost overlapping results. On the contrary, different expressions of $j^\mu(\vec{r})$ derived making use of the Gordon decomposition¹⁶, the socalled CC1 and CC2 currents, may give up to 10% difference in the extracted spectroscopic factors¹⁸.

With increasing Q^2 and ω a relativistic approach becomes necessary. The bound state wave function Ψ_i is now a four-spinor. In today's calculations it is obtained within a Dirac-Hartree mean-field approximation of the many-body problem. Scalar (S) and vector (V) optical potentials in a Dirac equation for Ψ_f describe the interaction of the ejectile with the rest of the nucleus and are responsible for spinor distortion of the final state with respect to the free case. This relativistic DWIA is thus based on (relativistic) IPSM wave functions.

The presence of negative-energy components in the bound-state wave function destroys factorization already in the relativistic PWIA cross section^{19,20}. However, the most important relativistic effects are due to the replacement $E + M \rightarrow \tilde{E} + \tilde{M} = (E - V) + (M + S)$, with V positive and S negative. This produces an overall reduction due to the spinor normalization factor $(E + M)/2E$ and an enhancement of the low components of the bound state wave function. This has two consequences. First, the strength of the

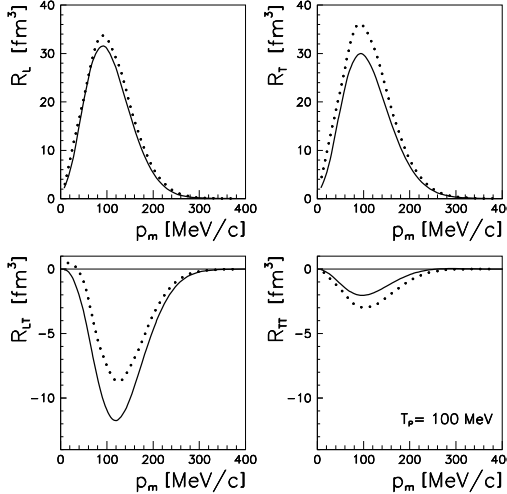


Figure 1. Separated structure functions for the reaction $^{16}\text{O}(\text{e},\text{e}'\text{p})^{15}\text{N}_{\text{g.s.}}$ with an emitted proton with 100 MeV kinetic energy. Solid (dashed) lines are relativistic (nonrelativistic) results (from Ref. ²³).

peak of the momentum distribution at low p -values (≤ 300 MeV) is reduced and correspondingly the extracted spectroscopic factors are increased (by $\sim 10 - 15\%$, as already estimated through the socalled Darwin term ²¹). Second, the shape at high p -values (≥ 300 MeV) is also modified. In addition, as the low components also depend on a $\vec{\sigma} \cdot \vec{p}$ factor, a different behaviour is expected for the spin-orbit partner shells, $j = l \pm \frac{1}{2}$, with a major sensitivity in R_{LT} and the left-right asymmetry, larger for the jack-knifed $j = l - \frac{1}{2}$ (e.g. $p_{1/2}$ in ^{16}O) than for the stretched $j = l + \frac{1}{2}$ (e.g. $p_{3/2}$) (see Ref. ²²).

The relevance of genuine relativistic effects has recently been investigated ²³ in a consistent comparison between nonrelativistic and relativistic calculations. Significant relativistic effects, especially in R_T and R_{LT} , are found already for a proton kinetic energy as low as 100 MeV (Fig. 1).

In the kinematics of Ref. ⁵, i.e. $Q^2 = 0.8 \text{ GeV}^2$ and $\omega = 439 \text{ MeV}$, relativity is quite important to describe the ^{16}O data ^{24,25}. It is remarkable that the extracted spectroscopic factors are in this case much larger than those obtained at lower Q^2 , i.e. $S_{p_{1/2}} = 0.73$ and $S_{p_{3/2}} = 0.71$ in Ref. ²⁴, and $S_{p_{1/2}} = 0.72$ and $S_{p_{3/2}} = 0.67$ in Ref. ²⁵. However, one has also to observe that the data of Ref. ⁵ for the first time are given directly in terms of cross sections, not (model dependent) reduced cross sections.

2.2 Transparency

The (e,e'p) reaction under quasi-free kinematics is also a valuable tool to study nucleon propagation in the nuclear medium. Data are available for Q^2 up to 7 GeV² on a variety of target nuclei²⁶. A systematic study has recently been accomplished¹⁰ for proton kinetic energies in the range between 300 and 1800 MeV that includes the minimum of the nucleon-nucleon total cross section and its rapid rise above the pion production threshold. These features are partially reflected in the energy-dependent attenuation of the proton flux. This attenuation is measured by the transparency ratio

$$T = \frac{\int_{\Delta E} dE \int_{\Delta \vec{p}} d\vec{p} \sigma_{\text{exp}}(\vec{p}, E)}{\int_{\Delta E} dE \int_{\Delta \vec{p}} d\vec{p} \sigma_{\text{PWIA}}(\vec{p}, E)}, \quad (3)$$

where ΔE and $\Delta \vec{p}$ define the range of missing energy and momentum explored by the experiment. In the data analysis a factorized expression is assumed both for σ_{exp} and σ_{PWIA} and, apart from kinematics, relativity is ignored in the calculation of σ_{PWIA} . Thus T is a heavily model dependent quantity. However, the role of genuine attenuation of FSI with increasing energy must be understood before studying other mechanisms, such as e.g. color transparency.

In fact, FSI at high energy are described in the eikonal or Glauber approximation²⁷. The multiple scattering of the ejected proton can also be described semiclassically within the intranuclear cascade model²⁸. This model has the advantage of directly implementing the detector acceptances that limit the range of ΔE and $\Delta \vec{p}$. In contrast, the eikonal approximation allows for a detailed analysis of the contribution of each shell to the integrated transparency as well as to its angular distribution²⁸. It is remarkable that quite similar results are obtained with the two approaches in good agreement with experiment by simply assuming a full occupation of the IPSM states. This is confirmed in the Glauber approach of Ref.²⁷ where no quenching of S_α is found and the role of short-range correlations is shown to be insignificant.

A possible Q^2 -dependence of spectroscopic factors, jumping from values around 0.6–0.7 at low Q^2 to unity at $Q^2 \geq 1$ GeV², simply means that something is not under control in either experiment or theory or both. One certainly should measure exclusive cross sections instead of providing (model dependent) reduced cross sections or transparencies. On the theory side a consistent approach is desirable, where relativity and FSI interactions are appropriately taken into account in calculating an unfactorized cross section. In particular, spin-orbit effects should be investigated.

2.3 Polarization observables

The measurement of proton polarization is simpler than the separation of the (polarized) structure functions and less affected by experimental errors, as it is obtained through the determination of asymmetries. With polarized incident electrons and polarized recoiling nucleons with spin directed along \hat{s} the cross section for a proton detected in the solid angle $d\Omega_p$ in coincidence with the electron of energy E' scattered in $d\Omega'$ can also be written

$$\frac{d^3\sigma}{dE' d\Omega' d\Omega_p} = \frac{1}{2}\sigma_0 \left[1 + \vec{P} \cdot \hat{s} + h \left(A + \vec{P}' \cdot \hat{s} \right) \right], \quad (4)$$

where σ_0 is the unpolarized differential cross section, \vec{P} the outgoing nucleon polarization, h the electron helicity, A the electron analyzing power, and \vec{P}' the polarization transfer. In coplanar kinematics, only the component P^N of \vec{P} normal to the scattering plane survives, and \vec{P}' lies within the scattering plane with components P'^L and P'^S , parallel (longitudinal) and perpendicular (sideways) to the outgoing proton momentum, respectively.

Without FSI, $P^N = 0$. Therefore P^N is a good candidate to look at when studying nuclear transparency, as its Q^2 dependence reflects the energy dependence of FSI. A first experiment has been performed on ^{12}C at MIT-Bates²⁹ for $(\omega, q) = (194, 756)$ MeV. Relativistic DWIA results are indeed sensitive

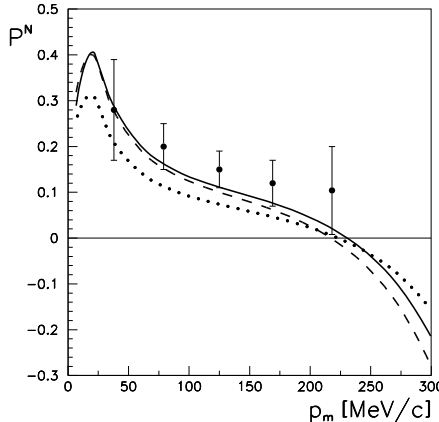


Figure 2. The induced polarization of the $p_{3/2}$ proton hole in the $^{12}\text{C}(\text{e}, \text{e}'\vec{p})$ reaction as a function of the missing momentum p_m . Data from Ref. ²⁹. Solid (dotted) line with the EDAD1 (EDAI-C) optical potential of Ref. ³⁰. Dashed line obtained with EDAD1 after removing the negative-energy components in the bound state (from Ref. ²³).

to the model used to simulate FSI. In Fig. 2 they are compared with data using two versions of an optical model potential based on empirical effective interactions³⁰. The role of relativity is appreciated by removing the negative-energy components in the bound state (dashed line), while sensitivity to FSI is shown by the difference between solid and dotted lines. In particular, these data are dominated by the real part of the spin-orbit optical potential^{29,31}.

Polarization transfer is a powerful technique to investigate the behaviour of the nucleon in vacuum and in the nucleus. The ratio P'^S/P'^L for a free proton is directly proportional to the ratio between the electric and magnetic form factors through a factor depending on the electron kinematics only:

$$\frac{G_E^p}{G_M^p} = -\frac{P'^S}{P'^L} \frac{E+E'}{2M} \tan(\frac{1}{2}\theta). \quad (5)$$

The two recoil polarization components were measured simultaneously up to 6 GeV^2 at JLab³² with the surprising result that the ratio (5) decreases linearly with Q^2 starting around 0.8 GeV^2 . This implies that G_E^p decreases much faster than the dipole form factor and nonrelativistically this means that the electric charge distribution in the proton extends to larger distances than the magnetization one. This trend is well reproduced in a chiral constituent-quark model where covariance is ensured in a point-form approach³³ (Fig. 3).

For a nucleon embedded in the nuclear medium one would expect some effects on the spatial distribution of its constituents due to the close proximity

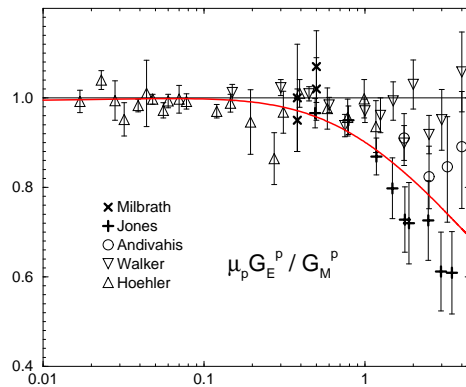


Figure 3. The ratio G_E^p/G_M^p rescaled by the theoretical proton magnetic moment μ_p in a (covariant) point-form approach with the Goldstone-boson-exchange quark model, compared to data as indicated (from Ref. ³³).

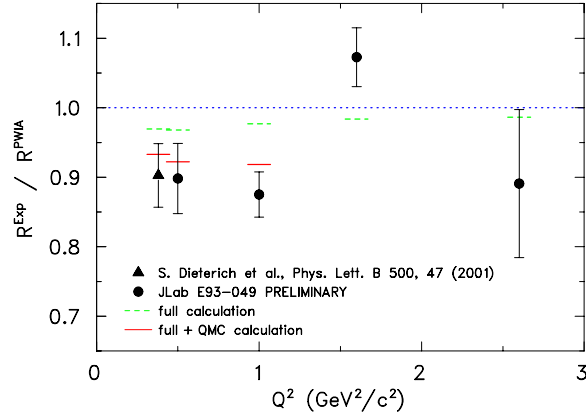


Figure 4. The observed super-ratio of Eq. (6) compared with the calculated one with (solid) and without (dashed) medium modified form factors. See text (courtesy of S. Dieterich).

of the other nucleons. To observe such effects the ratio R_T/R_L has been proposed, as for a free nucleon it is proportional to G_M^p/G_E^p . However, it has proven to be a very difficult task to disentangle changes of the nucleon structure from other conventional nuclear effects, such as meson-exchange currents, isobar configurations and FSI, because the nucleon form factors of a bound nucleon are not observable (see Ref. ¹¹ and references therein).

Polarization observables are less sensitive to systematic uncertainties and model ambiguities than cross sections. In a first experiment ⁷ on ¹⁶O the ratio P'^S/P'^L at $Q^2 = 0.8$ GeV² has been found in good agreement with calculations based on the free proton form factors with an experimental uncertainty of about 18%. A more precise measurement involves the super-ratio

$$R = \frac{|P'^S/P'^L|_A}{|P'^S/P'^L|_p} \quad (6)$$

obtained by dividing the ratio P'^S/P'^L observed in proton knockout off a nucleus A by that observed in electron-proton elastic scattering. The observed R for a target ⁴He nucleus is compared in Refs. ^{4,12} with results obtained with a variety of different models, including medium-modified proton form factors. The PWIA calculation (dotted horizontal line in Fig. 4) serves as baseline. The full relativistic calculation ³¹ predicts a reduced ratio, but cannot fully account for the measurement. The result up to $Q^2 = 1$ GeV² is in favour of some density-dependent form factor modification as predicted by the quark-meson coupling model of Ref. ³⁴. A proposal for a similar analysis on ¹⁶O is under discussion ³⁵.

3 (e,e'NN)

There is accumulating evidence for enhanced (e,e'p) transverse strength of non-single particle origin at high missing energies ^{36,11}. New data ⁶ on $^{16}\text{O}(\text{e},\text{e}'\text{p})$ cross section and separated responses at $Q^2 = 0.8 \text{ GeV}^2$ indicate a clear 1s peak at 40 MeV missing energy at small missing momenta p_m , but at larger p_m there is no peak and the DWIA knockout cross section becomes much smaller than the data. For $p_m > 200 \text{ MeV}$ the cross section is almost constant, (e,e'pp) and (e,e'pn) contributing by about one half of the measured cross section ³⁷. Besides testing the limits of the single-particle model in one-nucleon knockout ⁸, experiments are also proposed to directly observe two nucleons ejected in coincidence with the scattered electron.

Exclusive two-nucleon emission by an electromagnetic probe has been proposed long time ago ³⁸ to study nucleon-nucleon correlations. Due to the difficulty of measuring exceedingly small cross sections in triple coincidence, only with the advent of high-duty-cycle electron beams has a systematic investigation become possible. At present, only a few pioneering measurements have been carried out ^{39,40,41,2,42}, but the prospects are very encouraging.

The general theoretical framework involves the two-hole spectral density ^{43,1,44}, whose strength gives the probability of removing two nucleons from the target, leaving the residual nucleus at some excitation energy. Integrating the two-hole spectral density over the energy of the residual nucleus one obtains the two-body density matrix incorporating nucleon-nucleon correlations. The triple coincidence cross section is again a contraction between a lepton and a hadron tensor, which contains the two-hole spectral density through bilinear products of hadron currents J^μ of the type (2) suitably adapted to a final state with two ejected nucleons. FSI in principle require the solution of a three-body problem in the continuum. Thus one usually approximate FSI by an attenuated flux of each ejectile due to an optical model potential.

Even without FSI the two-hole spectral density is not factorized in the triple coincidence cross section. This makes a difficult task to extract information on correlations from data, and models are required to investigate suitable kinematic conditions where the cross section is particularly sensitive to correlations. *A priori* one may envisage that two-nucleon knockout is due to one- and two-body currents. Of course, one-body currents are only effective if correlations are present so that the nucleon interacting with the incident electron can be knockout together with another (correlated) nucleon. In contrast, two-body currents, typically due to meson exchanges and isobar configurations, lead naturally to two-nucleon emission even in an independent-particle shell model.

Two-body currents are mainly transverse and preferentially involve a proton-neutron pair. Thus reactions like (γ, pn) and $(e, e' pn)$ are particularly sensitive to their effects. In contrast, $(e, e' pp)$ reactions, where two-body currents play a minor role, are better suited to look for correlations, and resolution of discrete final states has been shown to provide an interesting tool to discriminate between contributions of different mechanisms responsible for two-nucleon emission ⁴⁶.

The shape of the angular distribution of the two emitted nucleons mainly reflects the momentum distribution of their c.m. total angular momentum L inside the target nucleus. When removing two protons from the ^{16}O ground state, the relative 1S_0 wave of the two protons is combined with $L = 0$ or 2 to give 0^+ or 2^+ states of the residual ^{14}C nucleus, respectively, while the relative 3P waves occur always combined with a $L = 1$ wave function giving rise to $0^+, 1^+, 2^+$ states. Combining the reaction description of Ref. ⁴⁴ with the many-body calculation of the two-particle spectral function in ^{16}O of Ref. ⁴⁵, in Ref. ⁴⁶ the cross section for the 0^+ ground state, and to a lesser extent also for the first 2^+ state of ^{14}C , was shown to receive a major contribution from the 1S_0 knockout. Such transitions are therefore most sensitive to short-range correlations. This is indeed the case, as seen in two exploratory studies performed at NIKHEF ^{39,40}, and confirmed in Ref. ⁴¹. As the calculations give significantly different results for different correlation functions, precise data could give important constraint when modelling the off-shell behavior of the nucleon-nucleon potential.

Superparallel kinematics has been preferred at Mainz ⁴², with one proton ejected along the virtual photon direction and the other in the opposite direction. In this kinematics only the pure longitudinal and pure transverse structure functions occur in the cross section, and a Rosenbluth L/T separation becomes possible. The effect of two-body currents is further suppressed by looking at the longitudinal structure function that is most sensitive to short-range correlations. The data are still preliminary and require further analysis before a fully reliable comparison with calculations can be done. Nevertheless they show distinctive features predicted by calculations ^{46,47}.

Tensor correlations are expected to play a major role in $(e, e' pn)$ reactions where, however, the proton-neutron pair is ejected by a much more complicated mechanism involving two-body currents. In the superparallel kinematics of the proposed Mainz experiment ³ with $(\omega, q) = (215, 316)$ MeV the predicted cross sections for $(e, e' pn)$ are about one order of magnitude larger than the corresponding cross sections for $(e, e' pp)$ reactions ⁴⁹. This enhancement is partly due to meson-exchange currents and partly to tensor correlations. Quite different results are predicted depending on these correlations being

included or not. An accurate determination of the two-hole spectral density is thus most desirable in order to disentangle the effects of two-body currents from those of nuclear correlations.

Experimentally, additional and precise information will come from measurement of the recoil polarization of the ejected proton in either $(e,e'pp)$ or $(e,e'pn)$. Resolving different final states is a precise filter to disentangle and separately investigate the different processes due to correlations and/or two-body currents. The general formalism is available ⁴⁸ and has been extended to study polarization observables also in the case of two nucleons emitted by a real photon ⁵⁰.

4 Conclusions

The advent of high-energy continuous electron beams coupled to high-resolution spectrometers has opened a new era in the study of basic nuclear properties such as single-particle behaviour and nucleon-nucleon correlations by means of one- and two-nucleon emission. In parallel new relativistic theoretical approaches have been developed showing that relativistic effects are most important and affect the interpretation of data even at moderate energies of the emitted particles. A striking feature coming out of the present analysis of $(e,e'p)$ world data is an apparent Q^2 dependence of the extracted spectroscopic factors. This is clearly not acceptable and indicates that something is missing in the theoretical treatment of the reaction mechanism. However, it is also rather important to measure cross sections directly without introducing a model-dependent treatment of data as was done in the past at low Q^2 in order to produce reduced cross sections or at high Q^2 when looking at the nuclear transparency.

Polarization observables are most useful to gain information about hadron currents and final-state interactions. As the normal recoil polarization P^N vanishes without FSI, its Q^2 dependence in exclusive $(e,e'p)$ reactions deserves a detailed study in connection with the problem of nuclear transparency and, ultimately, of color transparency. Measuring the components of the induced (transfer) polarization, on the other side, gives important information about possible medium modification of the nucleon electromagnetic form factors. Ultimately, a complete determination of the scattering amplitudes is only possible with polarization measurements.

Exclusive experiments with two-nucleon emission in electron scattering require triple coincidences with three spectrometers. This is now possible and the first experiments have been performed. By an appropriate selection of kinematic conditions and specific nuclear transitions, it has been shown that

data are sensitive to nuclear correlations. In turn these strictly depend on the nucleon-nucleon potential. Therefore, two-nucleon emission is a promising field deserving further investigation both experimentally and theoretically in order to solve a longstanding problem in nuclear physics.

In conclusion, it is clear that the field of electron scattering on complex nuclei offers a wide spectrum of still open problems in understanding the nuclear behaviour.

5 Acknowledgements

I would like to thank the organizers for a most pleasant workshop and their warm hospitality. I also would like to thank the Institute for Nuclear Theory at the University of Washington for its hospitality and the Department of Energy for partial support during the completion of this work.

References

1. S. Boffi, C. Giusti, F.D. Pacati and M. Radici, *Electromagnetic Response of Atomic Nuclei*, Clarendon Press, Oxford, 1996.
2. A1/1-97: G. Rosner and J. Friedrich, spokemen.
3. A1/5-98: P. Grabmayr and G. Rosner, spokemen.
4. S. Dieterich *et al.*, Phys. Lett. B 500, 47 (2001); A1/2-93: J. Friedrich, R. Ransome, G. Rosner and H. Schmieden, spokemen.
5. J. Gao *et al.*, Phys. Rev. Lett. 84, 3265 (2000); E-89-003: A. Saha, W. Bertozi, R.W. Lourie and L.B. Weinstein, spokemen.
6. N. Liyanage *et al.* (E-89-003), Phys. Rev. Lett. 86, 5671 (2001).
7. S. Malov *et al.*, Phys. Rev. C 62, 057302 (2000); E-89-033: C. Glashausser, C.C. Chang, S. Nanda and R. Rutt, spokemen.
8. E-00-102: A. Saha, W. Bertozi, L.B. Weinstein and K. Fissum, spokemen (an update to E89-003).
9. E-91-013: D. Geesaman, spokeman.
10. D. Abbott *et al.*, Phys. Rev. Lett. 80, 5072 (1998).
11. D. Dutta *et al.*, Phys. Rev. C 61, 061602(R) (2000).
12. E-93-049: J. van den Brand, R. Ent and P.E. Ulmer, spokemen.
13. S. Boffi, C. Giusti and F.D. Pacati, Phys. Rep. 226, 1 (1993).
14. A. Polls *et al.*, Phys. Rev. C 55, 810 (1997).
15. L. Lapikás *et al.*, Phys. Rev. C 61, 064325 (2000).
16. T. de Forest, Nucl. Phys. A 392, 232 (1983).
17. J.J. Kelly, Phys. Rev. C 56, 2672 (1997).
18. J.M. Udías *et al.*, Phys. Rev. C 64, 024614 (2001).

19. S. Gardner and J. Piekarewicz, Phys. Rev. C 50, 2822 (1994).
20. J.A. Caballero *et al.*, Nucl. Phys. A 632, 323 (1998).
21. S. Boffi *et al.*, Nuovo Cim. A 98, 291 (1987).
22. J.A. Caballero *et al.*, Nucl. Phys. A 643, 189 (1998).
23. A. Meucci, C. Giusti and F.D. Pacati, Phys. Rev. C 64, 014604 (2001).
24. J.M. Udías *et al.*, Phys. Rev. Lett. 83, 5451 (1999).
25. J.J. Kelly, Phys. Rev. C 60, 044609 (1999).
26. D.F. Geesaman *et al.*, Phys. Rev. Lett. 63, 734 (1989); G. Garino *et al.*, Phys. Rev. C 45, 780 (1992); N.C.R. Makins *et al.*, Phys. Rev. Lett. 72, 1986 (1994); T.G. O'Neill *et al.*, Phys. Lett. B 351, 87 (1995).
27. L. Frankfurt, M. Strikman and M. Zhalov, Phys. Lett. B 503, 73 (2001).
28. Y.S. Golubeva *et al.*, Phys. Rev. C 57, 2618 (1998).
29. R.J. Woo *et al.*, Phys. Rev. Lett. 80, 456 (1998).
30. E.D. Cooper *et al.*, Phys. Rev. C 47, 297 (1993).
31. J.M. Udías and J.R. Vignote, Phys. Rev. C 62, 034302 (2000).
32. M.K. Jones *et al.*, Phys. Rev. Lett. 84, 1398 (2000); E-99-007: E. Brash, M. Jones, G.F. Perdrisat and V. Punjabi, spokemen.
33. R.F. Wagenbrunn *et al.*, Phys. Lett. B 511, 33 (2001).
34. D.H. Lu *et al.*, Phys. Rev. C 60, 068201 (1999).
35. PR-01-013: S. Strauch, E. Brash, C. Glashausser and R. Ransome, spokemen.
36. P.E. Ulmer *et al.*, Phys. Rev. Lett. 59, 2259 (1987); R.W. Lourie *et al.*, Phys. Rev. C 57, R444 (1993); M. Holtrop *et al.*, Phys. Rev. C 58, 3205 (1998).
37. S. Janssen *et al.*, Nucl. Phys. A 672, 285 (2000).
38. K. Gottfried, Nucl. Phys. 5, 557 (1958).
39. C.J.G. Onderwater *et al.*, Phys. Rev. Lett. 78, 4893 (1997).
40. C.J.G. Onderwater *et al.*, Phys. Rev. Lett. 81, 2213 (1998).
41. R. Starink *et al.*, Phys. Lett. B 474, 33 (2000).
42. G. Rosner, Prog. Part. Nucl. Phys. 44, 99 (2000).
43. S. Boffi, in *Two-nucleon Emission Reactions*, ed. by O. Benhar and A. Fabrocini (ETS Editrice, Pisa, 1990), p. 87.
44. C. Giusti and F.D. Pacati, Nucl. Phys. A 615, 373 (1997).
45. W.J.W. Geurts *et al.*, Phys. Rev. C 54, 1144 (1996).
46. C. Giusti *et al.*, Phys. Rev. C 57, 1691 (1998).
47. J. Ryckebusch *et al.*, Phys. Lett. B 441, 1 (1998).
48. C. Giusti and F.D. Pacati, Phys. Rev. C 61, 054617 (2000).
49. C. Giusti *et al.*, Phys. Rev. C 60, 054608 (1999).
50. C. Giusti and F.D. Pacati, nucl-th/0102036.